Nanocrystallite Formation in Amorphous Titania Coatings

University of Padova/University of Florida IREU 2021

Phoebe McClincy, Penn State University
Mentors: Dr. Marco Bazzan and Giulio Favaro, University of Padova

13 August 2021

Nanocrystallite Formation in Amorphous Titania Coatings

University of Padova/University of Florida IREU 2021

Phoebe McClincy, Marco Bazzan, and Giulio Favaro

13 August 2021

The use of mirrors and lenses is integral to the functionality of gravitational-wave-detecting interferometry. Indeed, the interferometers used by LIGO, Virgo, and soon KAGRA are based upon the Michelson interferometer, an L-shaped instrument that is built using lasers and mirrors. The latter reflect the laser light up and down the arms of the interferometer, and as such, it is crucial to limit the noise that is produced in doing so. Noise can be caused due to a variety of reasons, including but not limited to seismic noise from the Earth, thermal noise, and quantum noise. Thermal noise is the result of heat fluctuations in electrons. Quantum noise is caused by the inherent uncertainty of quantum parameters. A specific type of quantum noise, called shot noise, is caused by the fact that electrons travel in a current discretely. In this project, we specifically are interested in limiting the amount of noise accumulated from the mirrors used in these interferometers. The mirrors stand to experience a great deal of noise, particularly thermal and quantum, if not controlled. We seek to alter these mirrors with an optical coating, a substance that will change the way the laser light is reflected from the mirror and will subsequently decrease noise. In this project, we notably observe the crystallization properties of titania (TiO_2), and how they change with respect to temperature. Five different annealing temperatures were tested for TiO_2: 330°C, 340°C, 350°C, 380°C, and 390°C. We analyze the parameters recovered from the x-ray spectra of TiO_2 following heat treatment, and subsequently build a crystallization kinetics analysis from them.

1 Introduction and Motivations

The LIGO, Virgo, and KAGRA (LVK) instruments are based upon the scheme of the Michelson interferometer, shown in Figure 1. That is, a beam of laser light is directed at a beam splitter; this divides the single beam into two separate, orthogonal beams. These new beams are directed toward a mirror, reflected back to the beam splitter, and recombined to produce an interference pattern. In the case of gravitational wave (GW) detection, constructive interference is produced if there is a GW detected, and destructive interference is produced if not.

However, the LVK's instruments have been modified to include Fabry-Perot cavities, shown in Figure 2, which allow for a longer "distance" traveled by the laser, resulting in a more sensitive instrument. This can be confirmed using the common equation which relates strain (h) to the length traveled by the laser light (L) and the change in length of the interferometer arms (ΔL):

$$hL = \Delta L. \tag{1}$$

Thus, a larger length traveled is proportional to a more noticeable (longer) change in length. This results in a more sensitive interferometer.

The mirrors used to create these Fabry-Perot cavities can result in a substantial amount of noise; the mirrors are created via a stack of alternating low and high-refractive index materials. These mirrors act as a Bragg grating, meaning that they reflect some wavelengths and transmit others. The Brownian noise caused by the high-index layers is one of the main sources of noise in the interferometer. As such, thermal treatments (specifically heating) are carried out to improve mechanical properties of the mirrors. This results in the formation of nanocrystals, which can prove to be detrimental to both mechanical and optical properties. This can, in turn, affect the overall sensitivity of the detector. The goal of this project is to learn how the crystallization process proceeds, specifically for titania (TiO_2), in order to understand the final distribution of nanocrystallites and how to apply this information to Virgo instrumentation.

2 Methods

Substrates coated in titania were placed into an x-ray diffraction (XRD) machine. This machine tests how x-rays diffract from the material. As shown

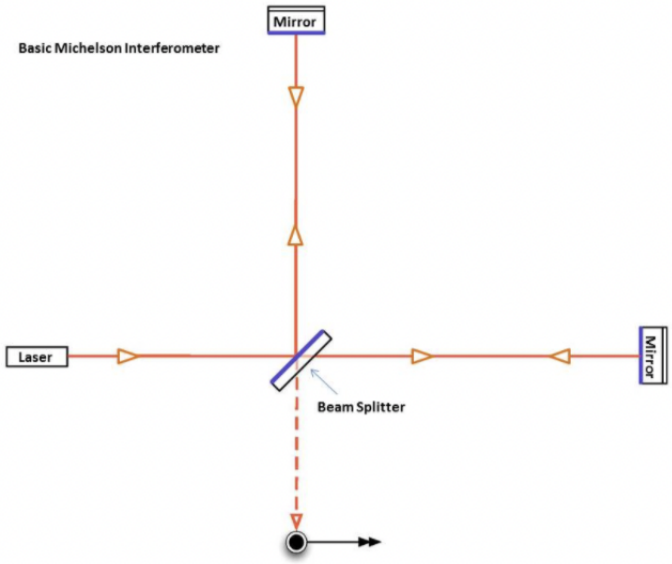

Figure 1: Schematic of the Michelson interferometer. [1]

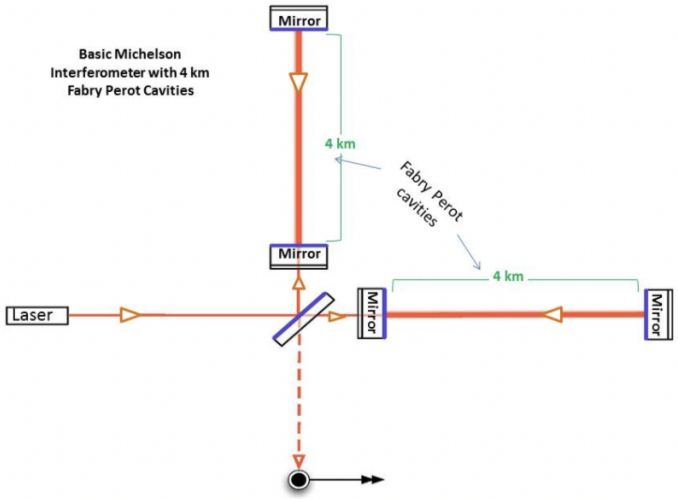

Figure 2: Schematic of the interferometer, including Fabry-Perot cavities. [1]

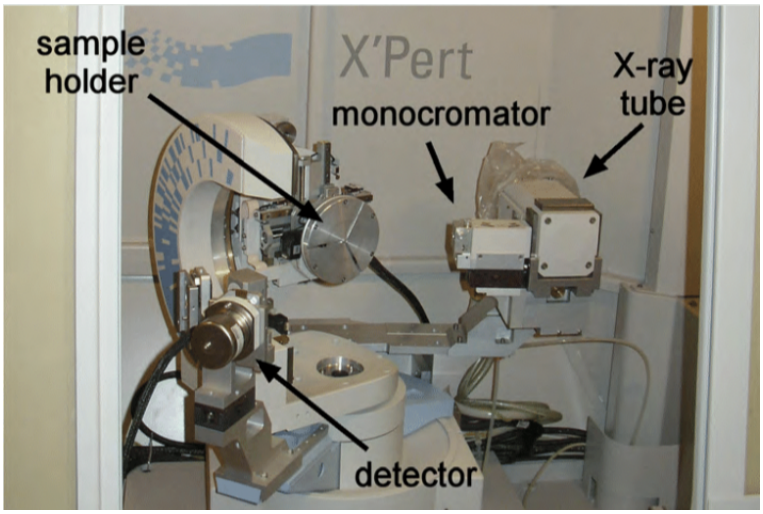

Figure 3: Diagram of the XRD machine. [2]

in Figure 3, the machine consists of a sample stage/holder (upon which the sample is mounted), an x-ray tube (which emits the x-ray), and a detector.

The detector scans in 2θ to obtain the x-ray spectrum, instead of simply θ. This is due to Bragg diffraction, shown in Figure 4. The scattering occurs at an angle of 2θ with respect to the incident beam. We measure this exiting angle of 2θ in our scans.

When the sample is placed into the XRD machine, a series of calibrations and alignments must occur to be sure that the machine is correctly placed. Manual scans are performed until we see what is expected for different positional parameters. When the machine is aligned, a program is implemented to scan the sample every so many seconds, the spectrum evolution is monitored as a function of time. The sample is heated from 25°C to a much hotter maximum temperature. (In our case, 5 temperatures tested: 330, 340, 350, 380, and 390°C). The sample cools and the final state of crystallization is observed in the x-ray spectrum.

3 Data Analysis

The data analysis was carried out using a program entitled Material Analysis Using Diffraction (MAUD) to perform a full-profile fitting using Rietveld's method. The measured parameters include the presence of different crystal

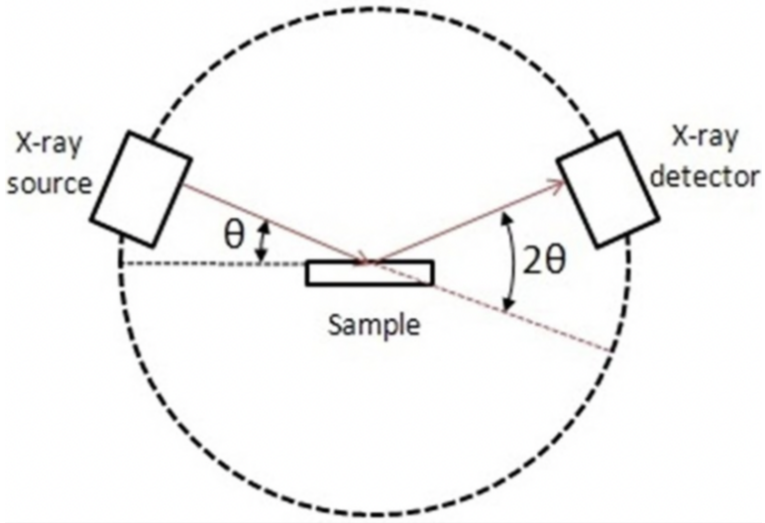

Figure 4: Bragg diffraction, in which the incident beam is diffracted at an angle of 2θ with respect to the incident beam itself. [3]

phases, lattice parameters A and C, and the average crystallite size. A sample x-ray spectrum and fit is shown in Figure 5.

The crystals in TiO_2 may appear in different phases: particularly, in this project, we are interested in the presence of phases anatase and rutile, shown in Figure 6. Anatase and rutile are, simply, different arrangements of the same atoms of TiO_2.

Shown in Figure 7, there are three principal phases of titania. Note that, at the temperatures we analyze in this project at standard pressure, we should observe only the presence of anatase.

4 Results

Although anatase should be the only observed phase, rutile was observed in excess of 10 percent weight of the final crystallized sample, shown in Figure 8. This is significant. We do not understand why yet – this physically should not be possible. We know this result is not a data error because it is present in five different, discrete analyses. A stressed state could lead to presence of *anatase* at a different temperature than expected, but this still does not explain why we see rutile at a different temperature. Overall, this result

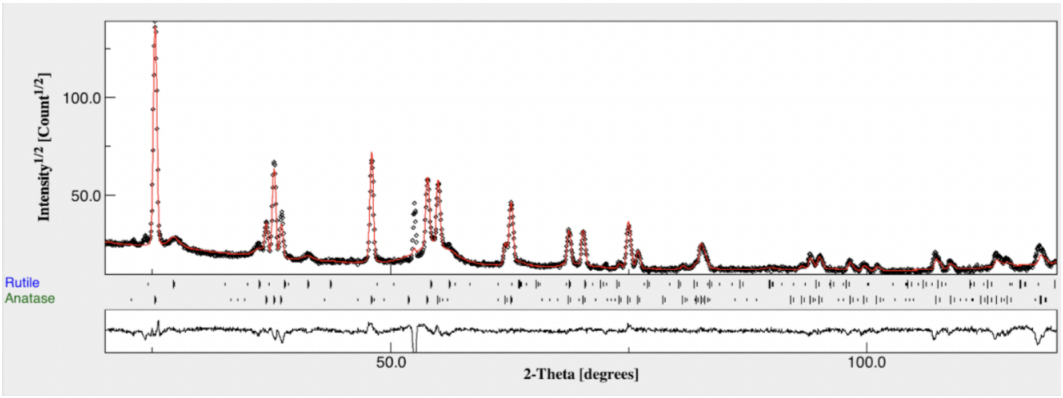

Figure 5: X-ray spectrum (black) and fit (red) for 390°C. The labels/tick marks at the bottom indicate which peaks are caused by which crystal phase, anatase or rutile.

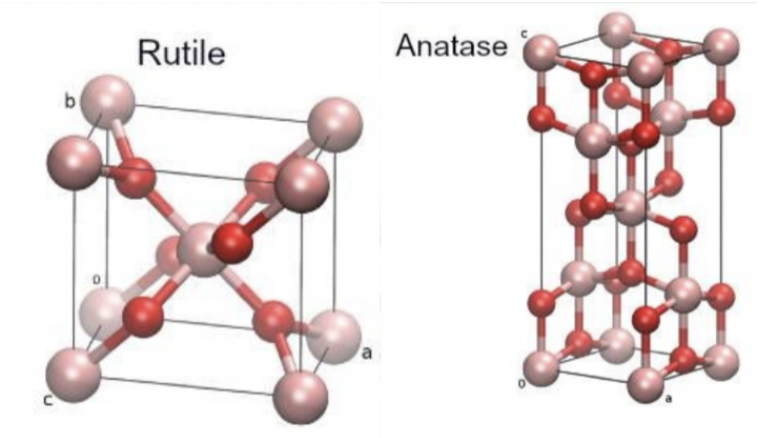

Figure 6: Anatase and rutile phases/atomic arrangements. [4]

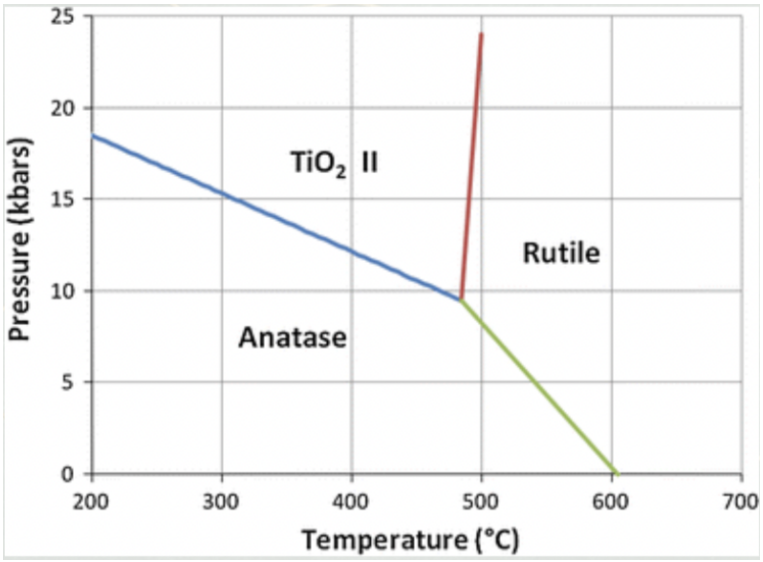

Figure 7: Phase diagram for titania. At standard pressure, and the temperatures we are analyzing, we should only observe the presence of anatase. [5]

proves to be very interesting, and opens the door for further exploration.

Final crystal size and the lattice parameters A and C, as a function of temperature, are shown in Figures 9 and 10/11, respectively.

The second part of the analysis and results for this project was based in crystallization kinetics theory. Firstly, we strive to obtain the nucleation rate from the crystal fraction. This is done by linearization. We begin with the crystal fraction x, a ratio equal to $V_{crystal}/V$, where V is the total volume of the sample and $V_{crystal}$ is the crystallized volume. x can be described as a function of time (t):

$$x(t) = 1 - e^{-\frac{4}{3}\pi\dot{n}v^3\frac{t^{3\alpha+1}}{3\alpha+1}}, \tag{2}$$

where $\dot{n}$ is the nucleation rate, v is the growth rate, and α is a constant. This is shown in Figure 12. Assuming that the crystallites are spherical and grow as a power law, we can consider x at small t and expand to first order:

$$x(t) = \frac{4}{3}\pi\dot{n}v^3\frac{t^{3\alpha+1}}{3\alpha+1}. \tag{3}$$

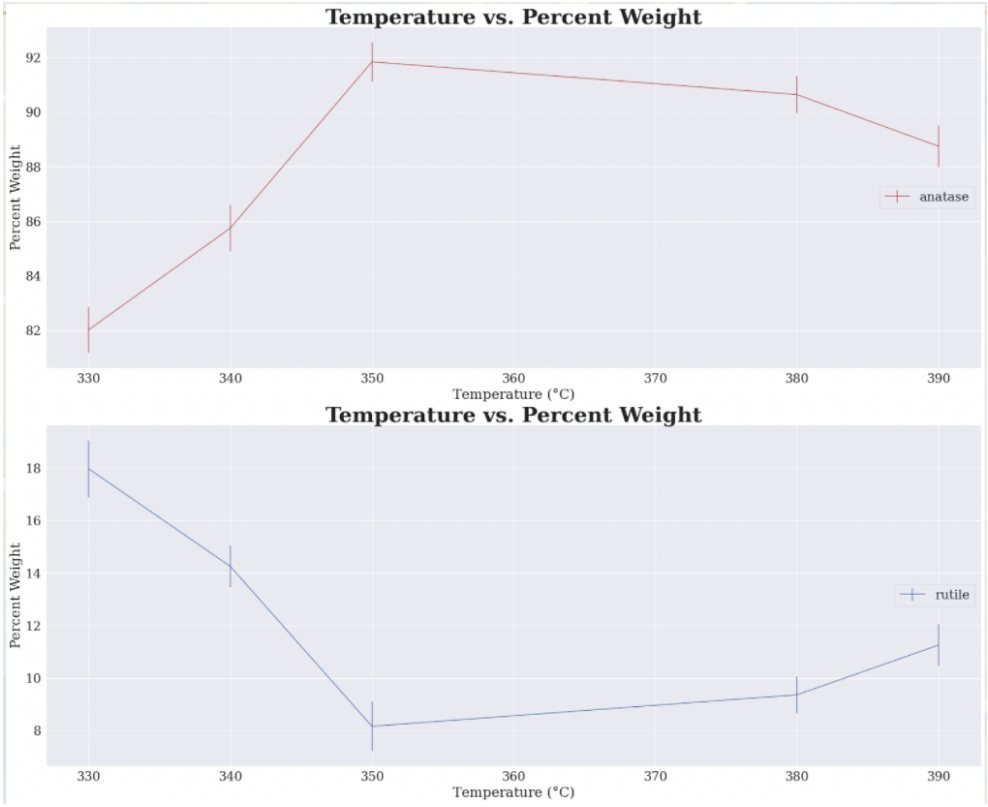

Figure 8: Percent weight for both anatase and rutile. The graphs trend opposite each other, as a function of temperature. The presence of rutile in excess of 10 percent weight of the final crystallized sample is unexplained for these temperatures at standard pressure.

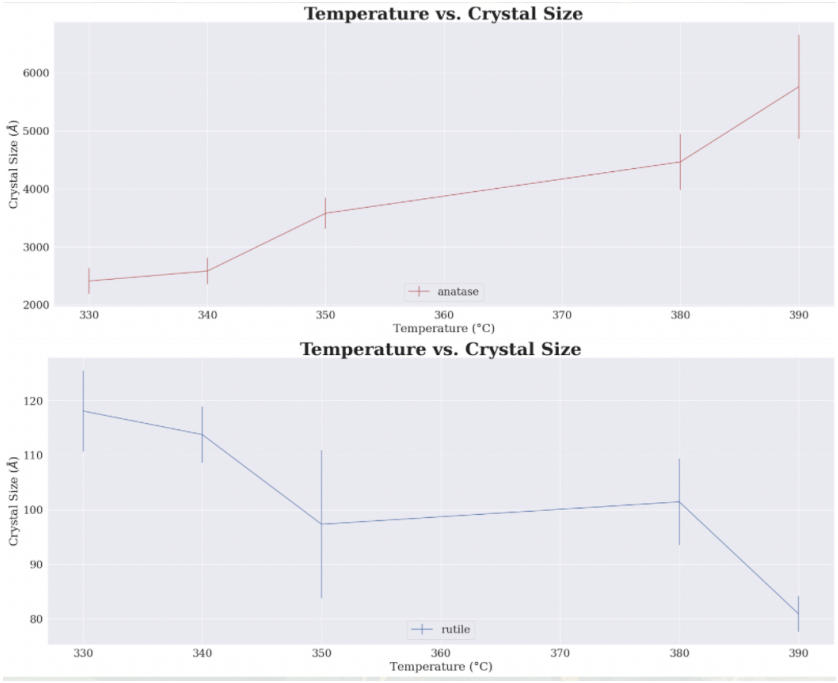

Figure 9: Final crystal size for anatase and rutile; the graphs trend opposite each other.

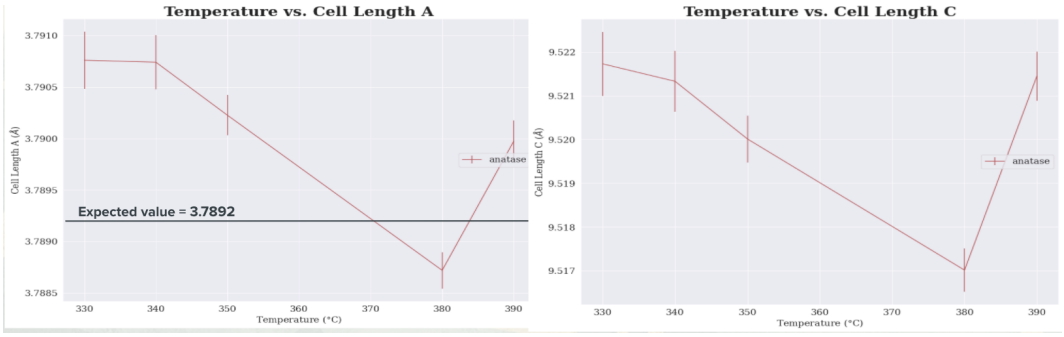

Figure 10: Anatase cell lengths A and C; the graphs show an outlier at 380°C. This may be due to instrumental error or analysis error, as well as sample error. The cause is unknown for sure. Overall, the values are consistent with the literature values for cell length A (3.7892 Å) and cell length C (9.537 Å). The black line indicates the literature value; the line is off the graph for cell length C.

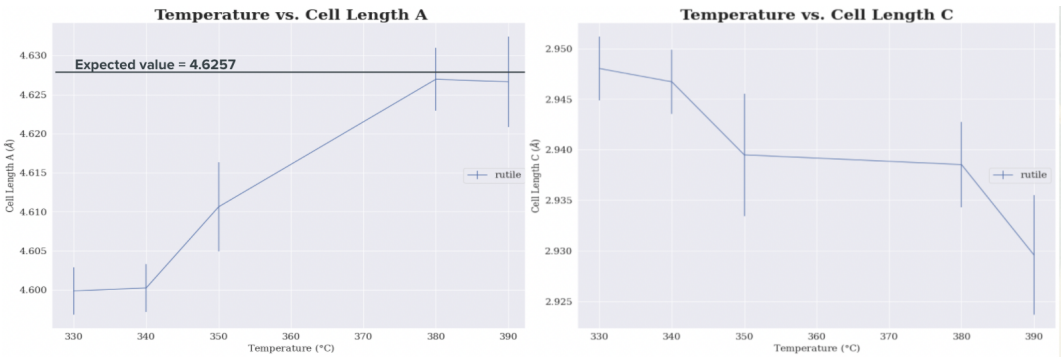

Figure 11: Rutile cell lengths A and C. Overall, the values are consistent with the literature values for cell length A (4.6257 Å) and cell length C (2.9806 Å). The black line indicates the literature value; the line is off the graph for cell length C.

Finally, we can consider three-dimensional growth, for which $\alpha = 1$, we find that

$$x(t) = \frac{\pi}{3}\dot{n}v^3t^4. \tag{4}$$

This equation can be rearranged:

$$\frac{x}{v^3} = \frac{\pi}{3}\dot{n}t^4. \tag{5}$$

Thus, the slope of this equation is proportional to the nucleation rate, shown in Figure 13.

Similarly, the mean radius $\bar{R}$ can be linearized to equal $\frac{vt}{2}$. Thus, the slope of the line is roughly equal to the growth rate v. This is shown in Figure 14.

The growth rate v is a function of temperature T:

$$v(T) = Ae^{\frac{-E_a}{k_BT}}, \tag{6}$$

where A and k_B are constants, and E_a is the activation energy. Linearized, this equation gives:

$$ln(v) = ln(A) - \frac{E_a}{k_BT}. \tag{7}$$

Thus, the slope of this plot is approximately equal to the activation energy, found here to be 669.806 kJ/mol, as shown in Figure **??**.

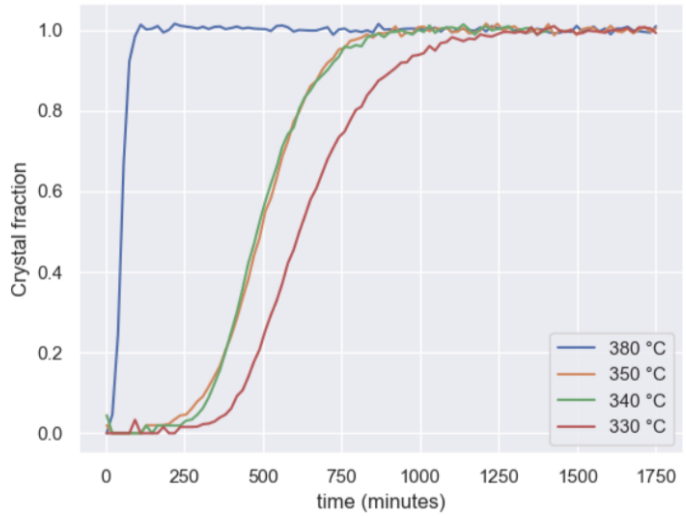

Figure 12: Crystal fraction as a function of time for different temperatures.

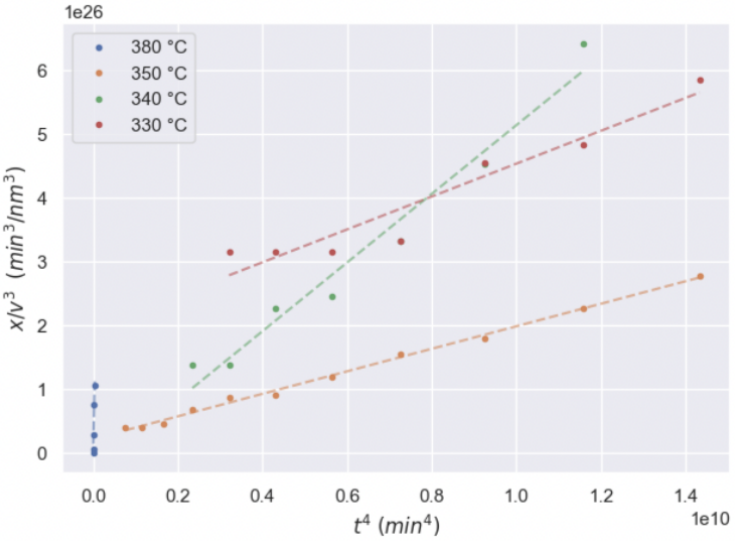

Figure 13: Crystal fraction as a function of t^4, for small times. The slopes of these lines are approximately equal to the nucleation rates for each temperature.

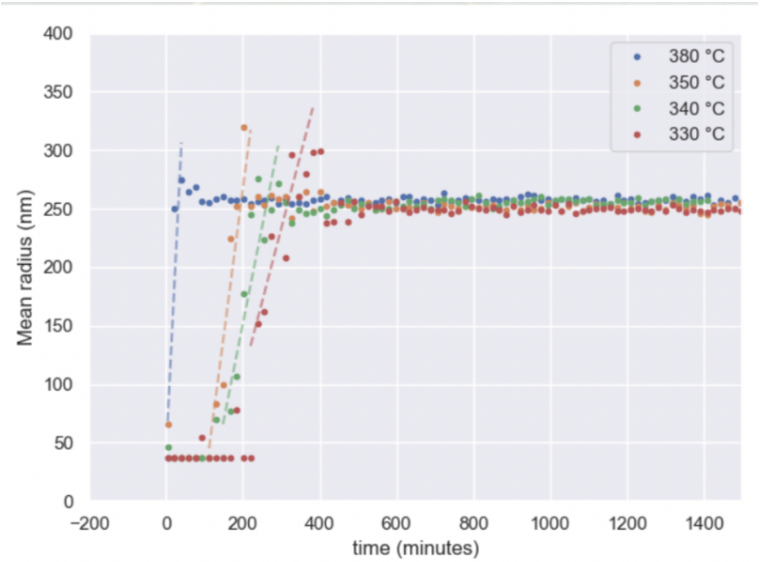

Figure 14: Mean radius, linearized for small times, as a function of time. The slope of the lines is approximately equal to the growth rate v.

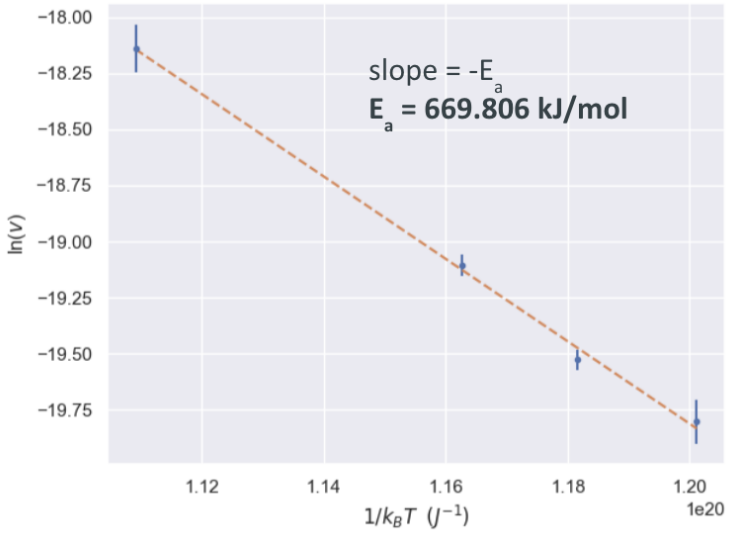

Figure 15: Arrhenius plot for the titania crystallization process. The activation energy was found to be equal to 669.806 kJ/mol.

5 Summary and Future Work

In summary, titania was annealed at five different temperatures, and the resulting crystallization was analyzed. We analyzed the crystal phases to obtain crystal parameters, and deduced the presence of the phase rutile in our experiment, although this should be impossible. This result opens a door to exploring why this result was obtained. Additionally, we used crystallization kinetics theory to obtain the growth rates and nucleation rates for each temperature. In the future, we may explore the presence of the rutile phase, or focus on testing the crystallization of other materials and applying those to Virgo science.

Funding for this experience was provided by NSF PHY-1950830 and NSF PHY-1460803.

References

[1] LIGO Laboratory, Caltech. n.d. *LIGO's Interferometer.*

[2] Ercolani, Daniele Sorba, Lucia. 2021. *Transport properties of InGaAs based devices.*

[3] Agiwaan, Hassan. 2014. *Thesis: Thermal Stability of cubic and nanocrystalline arc evaporated TiCrAlN coatings.*

[4] Janzeer, Yasmeen. 2013. *Surface Modification of Titanium and Titanium Alloys to Enhance Bone Healing.*

[5] Hanaor, D.A.H., Sorrell, C.C. 2011. *Review of the anatase to rutile phase transformation.*